Dictionary Learning based Low Dose Helical CT Reconstruction With Longitudinal TV Constraint

Yongyi Shi, Hengyong Yu, Yanbo Zhang, Rui Liu, Mannudeep Kalra, Ge Wang and Xuanqin Mou

***Abstract*— Multi-slice helical Computed Tomography (HCT) has been widely applied in clinical applications. Due to the potential radiation risk, it has attracted an increasing attention to reduce radiation dose while maintaining the diagnostic performance. Inspired by the longitudinal sampling inconsistencies of helical CT scanning, in this paper, we develop a statistical iterative reconstruction algorithm based on three-dimensional dictionary learning to improve image quality for low-dose HCT. The longitudinal Total Variation (TV) is added to change the image noise distribution. The classical distance-driven projection and back-projection models are employed to avoid artifact-inducing. To enhance the computational performance, Graphics Processing Unit (GPU) implementation, Order Subset technology and Nesterov's acceleration strategy are employed in our iterative reconstruction codes to accelerate the optimization. The Contrast Noise Ratio (CNR) index of reconstructed images and the subjective evaluation of medical practitioners all verify the superiority of our proposed algorithm.**

Keywords—low dose HCT; longitudinal constraint; dictionary learning; distance driven; GPU implementation

I. INTRODUCTION

Multi-slice helical Computed Tomography (HCT) has been widely used in clinical applications. With the increasing of helical CT scans, its potential radiation risk attracts increasingly public concerns. How to reduce radiation dose while maintaining the diagnostic performance is a hot topic in current CT field. Decreasing the X-ray flux towards each detector, which is usually implemented by adjusting the operating current of the X-ray tube, results in a reduced radiation dose. Analytic reconstruction algorithms such as filtered backprojection (FBP) have been extensively used for HCT image reconstruction because of their computational efficiency. These algorithms generally consider the cone-beam geometry by calculating equivalent image planes to minimize the error between the reconstruction plane and the projection ray paths in 2D back-projection step, such as ASSR [1], AMPR [2] or wFBP [3]. However, the reconstructed images suffers from noise and streaking artifacts which severely degrade image quality. While the performance of analytic reconstruction algorithms is insufficient for low-dose conditions, iterative techniques have a great potential to reconstruct better image quality with substantially reduced artifacts aided by certain prior information with the increased computational cost.

Considering the properties of received photon numbers on each detector cell in low dose cases, statistical iterative reconstruction (SIR) [4] optimizes the maximum-likelihood or penalized-likelihood function formulated according to the statistical characteristics of projection data, which promises high reconstruction quality from noisy projection data. Meanwhile, the addition of a stabilizing function in terms of a regularizer may further reduce noise and artifacts. It is very easy to incorporate some kinds of prior information of target images into the regularizer. This provides another tool to control image quality. Till now, many types of prior information have been proposed, including total variation (TV) [5], dictionary learning (DL) [6], and so on.

Considering the longitudinal sampling inconsistencies of helical scanning, in this paper, we develop a statistical reconstruction algorithm based on three-dimensional dictionary learning. The goal is to improve image quality of low-dose HCT by adding the longitudinal TV to change the noise distribution of the images. Our method consists of two components. The first component is the SIR routine that enforces the statistical knowledge of the projections. The second component is the dictionary penalty with the longitudinal TV as a prior information of the image space distribution. Furthermore, because the reconstruction accuracy is affected by mathematical affinity and similarity between the actual implementation of the forward and back-projection, the classical distance-driven model [7], which matched between the actual implementation of the forward projector and back-projector, is used to improve the performance of the entire iterative procedure. In the optimization procedure, we use a separable quadratic surrogate algorithm for Poisson loglikelihood function and Newton's gradient method for image update. Furthermore, the order subsets and the Nesterov's acceleration strategy [8] are used to accelerate the optimization. Besides, the proposed method is implemented in a Graphics Processing Unit (GPU) for efficient computing. The dataset supported by Low Dose CT Grand Challenge was employed to validate our proposed algorithm.

The rest of this paper is organized as follows. In the second section, the algorithm details are described. In the third section, the results are presented. Finally, some related issues are discussed and the conclusion is drawn.

This work was supported by the National Natural Science Foundation of China (NSFC) (No. 61571359) and National Key Research and Development Program of China (No. 2016YFA0202003).

YY Shi and XQ Mou are with the Institute of Image processing and Pattern recognition, Xi'an Jiaotong University, Xi'an, Shaanxi 710049, China; HY Yu, YB Zhang and R Liu are with Department of Electrical and Computer Engineering, University of Massachusetts Lowell, MA, 01854; M Kalra is with Department of Imaging, Massachusetts General Hospital, Harvard Medical School, Boston, MA, 02114; G Wang is with Department of Biomedical Engineering, Rensselaer Polytechnic Institute, Troy, NY, 12180; Corresponding author: XQ Mou (e-mail:xqmou@xjtu.edu.cn).

DOI: 10.12059/Fully3D.2017-11-3201035

II. METHODS

A. Statistical model

For HCT reconstruction, while the traditional methods of interpolating helical data to an equivalent plane can lead to inherently inaccuracies, the direct reconstruction methods based on a statistical model can explicitly describe practical applications more accurate. Let $\mu = (\mu_1, \cdots, \mu_J)^T \in \mathbb{R}_+^J$ be the discrete vector of linear attenuation coefficient. The SIR is equivalent to minimize the following objective function:

$$\Phi(\mu) = \sum_{i=1}^{I} \frac{w_i}{2} ([A\mu]_i - \hat{p}_i)^2 + R(\mu), \qquad (1)$$

where $[A\mu]_i = \sum_{j=1}^{J} a_{ij}\mu_j$ denotes line integrals through the imaging object, $A = \{a_{ij}\}$ is the system matrix, I and J are respectively the numbers of projections and voxels, $\hat{p}_i$ represents an estimated line integral, w_i is the statistical weight for each x-ray path which reflects the inherent variations in credibility of data, and $R(\mu)$ denotes a regularization term.

B. Distance driven forward and back-projection

The performance of an iterative CT reconstruction algorithm is strongly determined by the features of forward and back-projection models. Because the forward and back-projection are unified in the distance-driven model, it can avoid artifact-inducing approximations characteristic of some other methods. Therefore, we employ this distance-driven model to maximize SIR performance. The distance-driven approach in Fig.1 projects the horizontal and vertical boundaries (black dots) of image voxel and the detector cell boundaries (white dots) onto a common axis. The black squares are projected voxel boundaries, and the white squares are projected detector cells boundaries. The overlap (we calculate the lengths of overlap along the x (or y) direction and the z direction and then multiply them to get the area of overlap) between the interval defined by the projected boundaries of an image voxel and the one defined by the projected boundaries of a detector cell weights the contribution of the selected image voxel to the selected detector cell (and vice versa). The total contribution of voxel V with attenuation μ_V to the line integral p_D for detector D is given by the following updating equation:

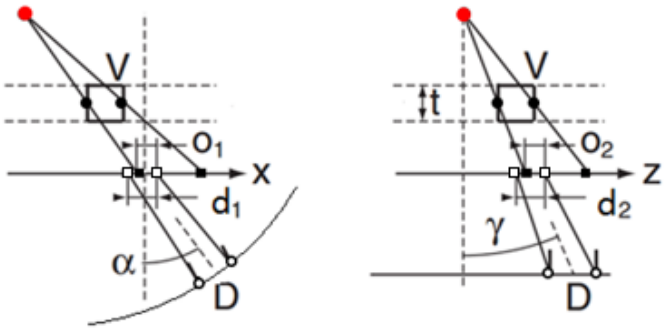

Fig. 1: Schematic representation of the distance-driven approach for forward projection (and back-projection) with cylindrical detectors.

$$p_D += \frac{t}{\cos\alpha\cos\gamma}\frac{o_1}{d_1}\frac{o_2}{d_2}\mu_V, \qquad (2)$$

where t is the isotropic voxel size, α and γ are the in- and out-of-plane angles of the line of interest with the y-axis, o_1 is the length of overlap and d_1 is the detector width in-plane, o_2 is the length of overlap and d_2 is the detector width out-of-plane.

C. Object function

The regularization term $R(\mu)$ in Eq.(1) represents prior information of the reconstructed image. It has been validated that the dictionary learning and sparse representation techniques are able to preserve fine structures and remove noise for low dose CT. With a predetermined dictionary D, the sparse representation can be obtained by solving the following minimization problem:

$$\min_{\alpha_s} \sum_s \|E_s\mu - D\alpha_s\|_2^2 + \gamma\|\alpha_s\|_0, \forall s \qquad (3)$$

where E_s denotes the extraction operator for the s^{th} data block which could be sparsely represented with a learned dictionary D and the associated coefficient are α_s, γ is the Lagrange multiplier, and $\|\alpha_s\|_0$ denotes the l_0 norm of the representation coefficients α_s which directly counts the number of the non-zero elements. In this work, the orthogonal matching pursuit (OMP) algorithm is used to find the sparse representation of each patch.

Taking into account the longitudinal sampling characteristics of helical scan mode, longitudinal TV constraints are employed. The longitudinal TV can be expressed as $TV_z(\mu) = \sum_{x,y,z}\sqrt{(\mu_{x,y,z} - \mu_{x,y,z-1})^2}$, where (x, y, z) represents the pixel index of the 3D image.

The image reconstruction process is equivalent to solve the following optimization problem:

$$\min_{\mu,\alpha_s} \sum_{i=1}^{I} \frac{w_i}{2}([A\mu]_i - \hat{p}_i)^2 + \beta\sum_s (\|E_s\mu - D\alpha_s\|_2^2 + \lambda\|\alpha_s\|_0) + \gamma TV_z(\mu), \qquad (4)$$

In this paper, the order subsets and the Nesterov's acceleration strategy are used to accelerate the optimization of iterative reconstruction. The number of subset is 16 and the total number of iterations is 5. Particularly, Eq. (4) can be iteratively optimized with a separable quadratic surrogate method.

D. GPU implementation

We implement the proposed algorithm on GPU to enhance its computational performance. To efficiently use memory and thread in a GPU kernel, four main functions are parallelized independently: 1) OMP algorithm 2) longitudinal TV 3)

forward projection and 4) back-projection. Nividia's Titan GPU and CUDA are used with Matlab. Main functions are implemented in Mex function of Matlab with CUDA.

III. Results

A. The datasets

The datasets generated by Low Dose CT Grand Challenge [9] are employed to validate our proposed algorithm. For the given 10 training datasets, projection data from z-flying focal spot technology [10] and FBP reconstructed images at both full and quarter dose are given. Hence, the images reconstructed by FBP at full dose are used as ground-truths. The lesion locations and type information are also given in the full-dose reconstructed images.

In this paper, the patient L067 is selected from the training datasets to demonstrate the merits of the proposed algorithm. The field of view of the reconstructed images is 34cm in diameter. In the patient L067, five different sizes and types of lesions are included. The locations of the lesions are indicated by red arrows in Fig. 2.

B. Image quality

Among the five lesions in Fig. 2, the third lesion is selected for visual inspection. Fig. 3 gives the reconstructed images by different methods. (a) is reconstructed by FBP at full dose (FD-FBP) to serve as ground truth; (b) is reconstructed by FBP at quarter dose (QD-FBP); and (c) is reconstructed by the TV-based SIR at quarter dose (QD-TVSIR); (d) is reconstruted by the DL-based SIR at quarter dose image (QD-DLSIR); and (e) is reconstructed by our proposed method at quarter dose.

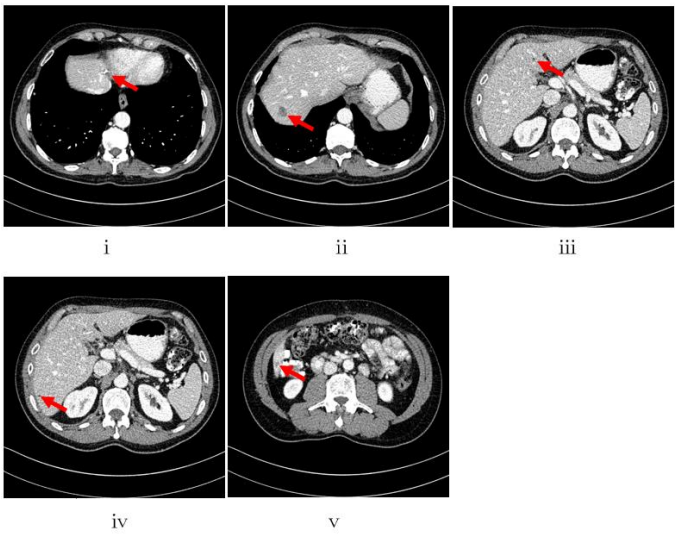

Fig. 2. Reconstructed images of patient L067 at full-dose using FBP. The lesions are indicated by red arrows. Among them, i is post op/post RFA (Radiofrequency Ablation) defect; ii and v indicate hemangioma; iii and iv indicate benign cyst. The display window is [-125 225] HU.

In Fig. 3(b), the imaging quality is severely degraded by noise and artifacts. Some details and important structures, such as the lesion and some blood vessels, cannot be discriminated. However, all of the iterative reconstruction methods can suppress the noise and artifacts in different degrees at quarter dose. Due to the piecewise constant assumption of TV, the lesion and some tiny blood vessels in Fig. 3(c) are obscure or invisible. In comparison, the DL-based SIR method could preserve the image detail and suppress noise. The lesion and blood vessels are easily discriminated in Fig. 3(d). By the effect of helical scanning, it makes the noise distribution inconsistent between transverse and longitudinal planes by simply using three dimensions dictionary constraints. This affects the image quality. In Fig. 3(e), the proposed method has a better performance both at suppressing noise and preserving image details.

To quantitatively evaluate the proposed method, in the same lesion, the same region of interest (ROI) is placed on lesion location as a low-constrast object and the adjacent liver as background (avoiding vessels). The CNR index are measured for all the iterative reconstructed images, which could be calculated as $\mathrm{CNR}=2\left|\mu_s-\mu_b\right|/(\sigma_s+\sigma_b)$, where μ_s and μ_b are the mean values in the signal and background, and σ_s and σ_b are the deviations of singla and background. The quantitative results of CNR are listed in Table Ⅰ. One can see that the proposed method achieves the best performance, which is coherent to the visual effects.

For subjective evaluation, the reconstructed images are evaluated by five readers with three years of experience. They are given a ROI showing the location of lesion. Each reader is asked to determine whether the lesion is present or absent, according to the following scoring system: 2 denotes very well identified, 1 denotes almost identified, 0 denotes possibly identified, -1 denotes probably identified, and -2 denotes not identified. The median score of five readers are summarized in Table Ⅱ. The proposed method also has a better performance at the detection of tiny lesions.

C. Computational cost

Our codes are run on an Nvidia's TitanX GPU and CUDA with Matlab. To focus on algorithm evaluation, we ignore the z-flying focal spot effect and use half of the projection from a determined focal spot. Meanwhile, only one GPU is utilized to run the code. Our codes are not optimized for better speed. To obtain a 512*512*288 image from 736*64 bins by 1152 views raw data, the computational costs of forward projection, back-projection, OMP algorithm and longitudinal TV algorithm are 65s, 77s, 133s and 2s, respectively, This is significantly faster than a CPU-based implementation. Using the order subsets and the Nesterov's acceleration strategy, the algorithm can converge after 5 iterations. Finally, we average the reconstructed images from different focal spot to make the final image.

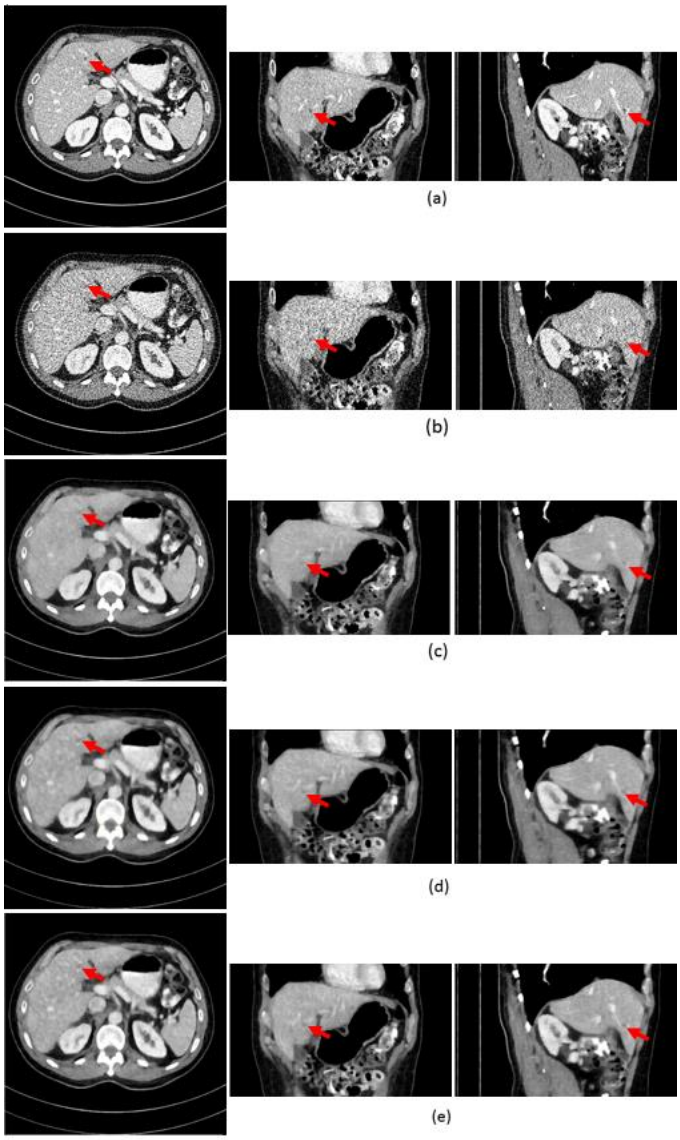

Fig. 3. Reconstructed 3D images of patient L067 at the third lesion by different methods. From left to right, the images are the transverse plane, the coronal plane and the sagittal plane, respectively. From (a) to (e), the images are reconstructed by the FD-FBP, QD-FBP, QD-TVSIR, QD-DLSIR and the proposed method, respectively. The display window is [-125 225] HU. The lesions are indicated by red arrows.

Table Ⅰ. The CNR of Different Lesions with Different Reconstructed Method.

Reconstruction method	Lesions				
	i	ii	iii	iv	v
QD-TVSIR	0.43	0.34	0.34	0.61	0.24
QD-DLSIR	0.78	0.61	0.31	0.89	0.26
Proposed Method	0.82	0.68	0.46	0.92	0.42

Table Ⅱ. Median Scores of Five Readers Evaluating Different Lesions with Different Reconstruction Method.

Reconstruction method	Lesions				
	i	ii	iii	iv	v
QD-TVSIR	-2	2	-1	-2	0
QD-DLSIR	-1	2	0	0	1
Proposed Method	-1	2	1	1	1

IV. DISCUSSIONS AND CONCLUSIONS

Considering the longitudinal characteristic, in this paper, a helical CT iterative reconstruction method is developed for noise reduction of quarter dose CT. The proposed method outperforms the QD-TVSIR and QD-DLSIR in both quantitative and subjective measures. Considering the computational cost for the proposed algorithm, the main function is implemented in GPU mode, which is significantly improved the computational efficiency. In th near future, more comprehensive evaluations will be performed to evaluate the proposed method with different dose levels.

ACKNOWLEDGMENT

The authors would like to thank Dr. Cynthia McCollough at Mayo Clinic the American Association of Physicists in Medicine, and grants EB017095 and EB 017185 from the USA National Institute of Biomedical Imaging and Bioengineering for the dataset.

REFERENCES

[1] Kachelrieß M, Schaller S, Kalender W A. Advanced single-slice rebinning in cone-beam spiral CT[J]. Medical Physics, 2000, 27(4):754-772.

[2] Flohr T, Stierstorfer K, Bruder H, et al. Image reconstruction and image quality evaluation for a 16 - slice CT scanner[J]. Medical Physics, 2003, 30(5):832-845.

[3] Stierstorfer K, Rauscher A, Boese J, et al. Weighted FBP--a simple approximate 3D FBP algorithm for multislice spiral CT with good dose usage for arbitrary pitch.[J]. Physics in Medicine & Biology, 2004, 49(11):2209-2218.

[4] Thibault J B, Sauer K D, Bouman C A, et al. A three-dimensional statistical approach to improved image quality for multislice helical CT.[J]. Medical Physics, 2007, 34(11):4526.

[5] Sidky E, Pan X. Image reconstruction in circular cone-beam computed tomography by constrained, total-variation minimization.[J]. Physics in Medicine & Biology, 2008, 53(17):4777-4807.

[6] Xu Q, Yu H, Mou X, et al. Low-dose X-ray CT reconstruction via dictionary learning.[J]. IEEE Transactions on Medical Imaging, 2012, 31(9):1682-1697.

[7] De M B, Basu S. Distance-driven projection and backprojection in three dimensions.[J]. Physics in Medicine & Biology, 2004, 49(11):2463-2475.

[8] D. Kim, S. Ramani, and J. A. Fessler, "Accelerating X-ray CT ordered subsets image reconstruction with Nesterov's first-order methods," in Proc. Intl. Mtg. on Fully 3D Image Recon. in Rad. and Nuc. Med, pp. 22–5, 2013.

[9] http://www.aapm.org/GrandChallenge/LowDoseCT/.

[10] Flohr T G, Stierstorfer K, Ulzheimer S, et al. Image reconstruction and image quality evaluation for a 64 - slice CT scanner with z - flying focal spot[J]. Medical Physics, 2005, 32(8):2536-254